

Synthesis, crystal structures and Hirshfeld surface analysis of 1,4-dibenzyl-6-methyl-1,4-dihydro-quinoxaline-2,3-dione

Emine Berrin Cinar,^a Ayman Zouitini,^b Youssef Kandri Rodi,^b Younes Ouzidan,^c Jérôme Marrot,^d Damien Prim,^{d*} Necmi Dege^a and Eiad Saif^e

Received 16 June 2020

Accepted 19 July 2020

Edited by J. T. Mague, Tulane University, USA

Keywords: crystal structure; Hirshfeld surfaces; quinoxaline; hydrogen bonding.

CCDC reference: 1936664

Supporting information: this article has supporting information at journals.iucr.org/e

^aDepartment of Physics, Faculty of Arts and Sciences, Ondokuz Mayıs University, Samsun, 55200, Turkey, ^bLaboratoire de Chimie Organique Appliquée, Université Sidi Mohamed Ben Abdallah, Faculté des Sciences et Techniques, BP 2202, Fez, Morocco, ^cLaboratoire de Chimie Physique et Chimie Bio-organique, Faculté des Sciences et Techniques Mohammedia, Université Hassan II, Casablanca, BP 146, 28800, Mohammedia, Morocco, ^dInstitut Lavoisier de Versailles, UVSQ, CNRS, Université Paris-Saclay, 78035 Versailles, France, and ^eDepartment of Computer and Electronic Engineering Technology, Sana'a Community College, Sana'a, Yemen. *Correspondence e-mail: eiad.saif2016@gmail.com

The title quinoxaline molecule, C₂₃H₂₀N₂O₂, is not planar, the dihedral angle between the mean planes of the benzene rings being 72.54 (15)°. In the crystal, molecules are connected into chains extending parallel to (10 $\bar{1}$) by weak C—H···O hydrogen bonds. Weak C—H··· π interactions link the chains, forming a three-dimensional network structure. Hirshfeld surface analysis revealed that the most important contributions for the crystal packing are from H···H (48.7%), H···C/C···H (32.0%), H···O/O···H (15.4%), C···C (1.9%), H···N/N···H (1.1%) contacts.

1. Chemical context

Given their importance in the pharmaceutical, chemical and industrial fields, the synthesis of quinoxaline and its derivatives has been a goal of chemists in recent years. Quinoxaline derivatives find use as anticancer (Noolvi *et al.*, 2011), anti-malarial (Guillon *et al.*, 2004), antifungal (Xu & Fan, 2011), antiviral (Cai *et al.*, 2008) and anti-inflammatory (Yan *et al.*, 2007) agents. Some quinoxaline derivatives have also been reported to be corrosion inhibitors for steel in an acidic medium (Zouitini *et al.*, 2018, 2019; El Janati *et al.*, 2020). In this work, we report the synthesis and structure of the title compound obtained by the action of benzyl chloride on 6-methyl-1,4-dihydroquinoxaline-2,3-dione in the presence of potassium carbonate and a catalytic quantity of tetra-*n*-butylammonium bromide. A Hirshfeld surface analysis was also performed.

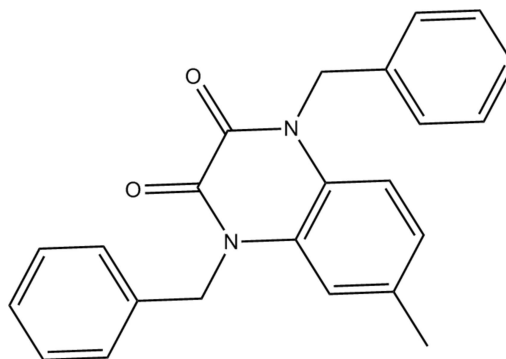
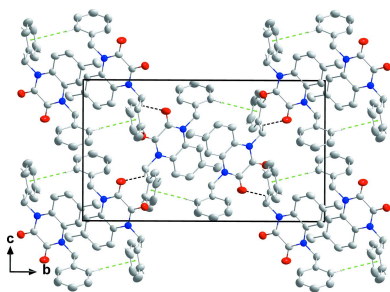


Table 1

Hydrogen-bond geometry (Å, °).

$Cg3$ is the centroid of the C11–C16 benzene ring.

$D-H\cdots A$	$D-H$	$H\cdots A$	$D\cdots A$	$D-H\cdots A$
C10–H10A \cdots O2 ⁱ	0.97	2.52	3.251 (3)	132
C16–H16 \cdots O1 ⁱ	0.93	2.55	3.3984 (4)	152
C25–H25 \cdots Cg3 ⁱⁱ	0.93	2.83	3.683 (3)	153

Symmetry codes: (i) $x - \frac{1}{2}, -y + \frac{1}{2}, z - \frac{1}{2}$; (ii) $-x + 2, -y, -z$.

2. Structural commentary

An *ORTEP* (Burnett & Johnson, 1996) view of the molecule is given in Fig. 1. The molecule is not planar, the dihedral angle between the mean planes of the benzene rings (C11–C16 and C24–C29) being 72.54 (15)°. The mean planes of the C1/N2/C9/C8/N1/C6 and C11–C16 rings make an angle of 73.093 (13)° while the C1–C6 and C24–C29 rings make an angle of 79.01 (14)°. The C1/N2/C9/C8/N1/C6 and C1–C6 rings are nearly coplanar, subtending a dihedral angle of only 3.07 (11)°. The C8=O1 and C9=O2 bonds show double-bond character with bond lengths of 1.222 (3) and 1.217 (3) Å, respectively. The N1–C10 and N2–C23 bond lengths are 1.476 (3) and 1.464 (3) Å, respectively while the C11–C10–N1 bond angle is 113.57 (18)° and the N2–C23–C24 bond angle is 114.05 (18)°. The C9–N2–C23 and C8–N1–C10–C11 torsion angles are –96.7 (2) and –93.4 (2)°, respectively.

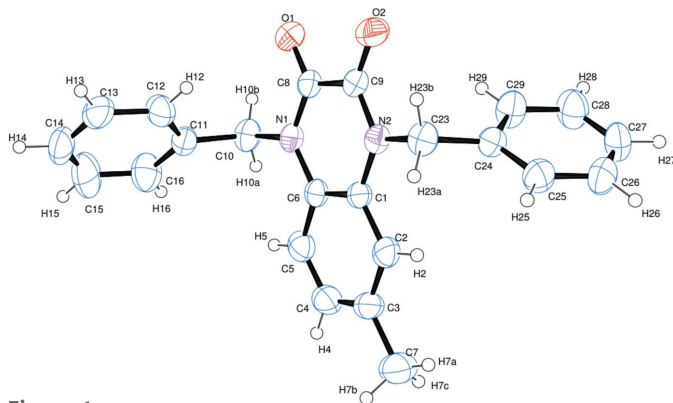


Figure 1

The molecular structure of the title compound. Displacement ellipsoids are drawn at the 40% probability level.

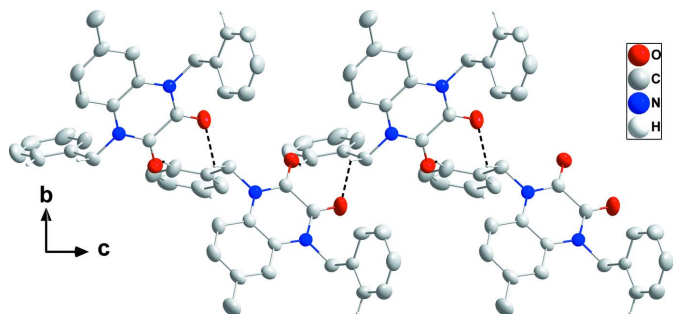


Figure 2

View of a portion of a chain along the a -axis direction with C–H \cdots O hydrogen bonds depicted by dashed lines.

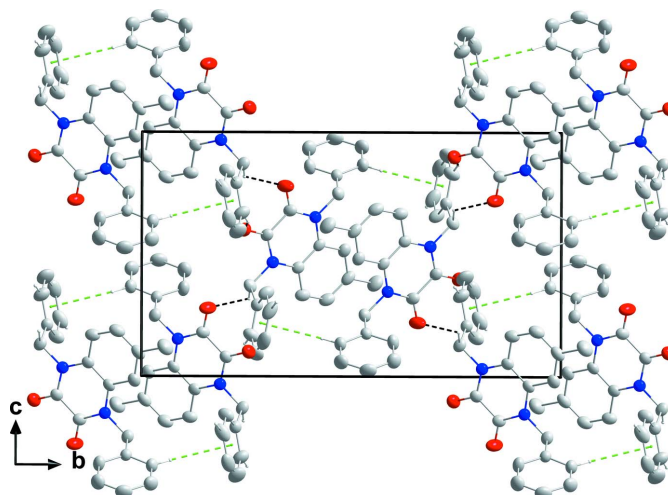


Figure 3

Packing viewed along the a -axis direction with C–H \cdots O hydrogen bonds and C–H \cdots π (ring) interactions depicted, respectively, by black and green dashed lines.

3. Supramolecular features

In the crystal, molecules are connected by weak C16–H16 \cdots O1 and C10–H10A \cdots O2 hydrogen bonds into chains extending parallel to (10 $\bar{1}$) (Table 1 and Fig. 2). Weak C25–H25 \cdots Cg3 interactions (2.83 Å; $Cg3$ is the centroid of the C11–C16 ring at $-x + 2, -y, -z$) link the chains into a three-dimensional network structure (Table 1 and Fig. 3).

4. Hirshfeld surface analysis

The *CrystalExplorer*17.5 (Turner *et al.*, 2017) program was used to analyse the interactions within the crystal. The donor–acceptor groups are visualized using a standard (high) surface resolution and d_{norm} surfaces mapped over a fixed colour scale of –0.140 (red) to 1.358 (blue) a.u., as illustrated in Fig. 4. Red spots on the surface of the d_{norm} plot indicate intermolecular contacts involving the hydrogen bonds. The red spots identified in Fig. 4(a) correspond to the intermolecular C–H \cdots O bonds. Regions close to the sum of the van der Waals radii are shown in white. Fig. 4(b) shows the shape-index surface, which can be used to detect the presence of π -stacking interactions.

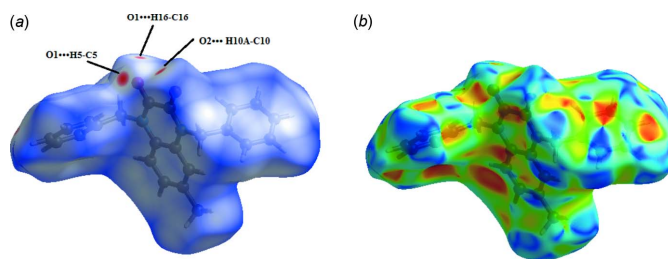


Figure 4

Hirshfeld surface mapper over (a) d_{norm} and (b) shape-index to visualize the interactions in the title compound.

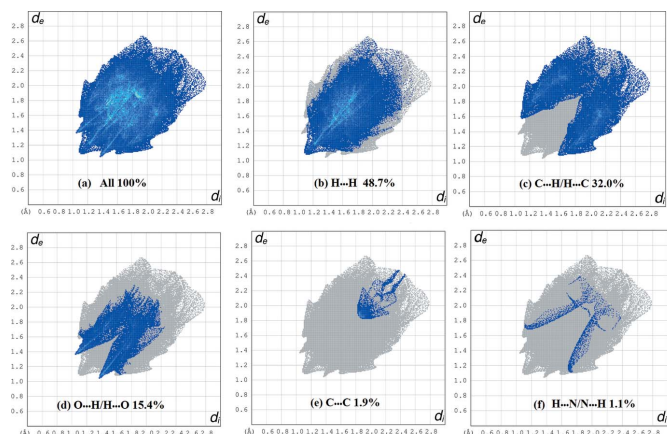


Figure 5
Fingerprint plot for all interactions and those delineated into the most important interactions.

The absence of characteristic triangles indicates that no significant π - π interactions are present. Two-dimensional fingerprints were also generated in the range -1 to 1 Å (Fig. 5). As expected, H...H (48.7%) and H...C/C...H (32.0%) contacts dominate the intermolecular interactions, but the O...H/H...O contacts are important directional intermolecular interactions in the crystal. The C...C (1.9%) and H...N/N...H (1.1%) contribute minimally to the overall crystal packing.

5. Database survey

A search of the Cambridge Structural Database (CSD, version 5.40, update August 2019; Groom *et al.*, 2016) using 1-benzyl-3,4-dihydroquinoxalin-2(1H)-one as the main skeleton revealed the presence of three structures similar to the title compound, but with different substituents. These are: 1,4,6-tribenzoyl-3-(4-bromobenzyl)-1,4-dihydroquinoxaline-2-one (LEQWIO; Abraham *et al.*, 2006), 1,4-dibenzoyl-6-trifluoromethyl-3-(4-bromobenzyl)-1,4-dihydroquinoxaline-2-one (LEQWOU; Abraham *et al.*, 2006) and 1,4-dibenzyl-6-chloro-1,4-dihydroquinoxaline-2,3-dione (PAWFEB; El Janati *et al.*, 2017). In the latter study (PAWFEB) examining compounds having the same skeletal system as the 1,4-dihydroquinoxaline-2,3-dione structure in the title compound, the corrosion inhibition efficiency of 1,4-diallyl-6-chloroquinoxaline-2,3-(1H,4H)-dione and 1,4-diallyl-6-nitroquinoxaline-2,3-(1H,4H)-dione on mild steel (MS) in 1.0 M HCl solution was investigated.

6. Synthesis and crystallization

To a solution of 6-methyl-1,4-dihydroquinoxaline-2,3-dione (0.3 g, 1.73 mmol) in DMF (15 mL), were added potassium carbonate (0.47 g, 3.61 mmol) and tetra-*n*-butylammonium bromide (0.07g, 0.23 mmol). After stirring for 10 min, 0.5 mL (4.32 mmol) of benzyl chloride was added and the mixture was stirred at room temperature for 6 h. After filtration of the salts, the DMF was evaporated under reduced pressure and

Table 2
Experimental details.

Crystal data	
Chemical formula	C ₂₃ H ₂₀ N ₂ O ₂
<i>M_r</i>	356.41
Crystal system, space group	Monoclinic, <i>P</i> ₂ ₁ / <i>n</i>
Temperature (K)	296
<i>a</i> , <i>b</i> , <i>c</i> (Å)	9.0844 (12), 18.7227 (18), 11.2708 (14)
β (°)	104.848 (4)
<i>V</i> (Å ³)	1853.0 (4)
<i>Z</i>	4
Radiation type	Mo <i>K</i> α
μ (mm ⁻¹)	0.08
Crystal size (mm)	0.30 × 0.16 × 0.06
Data collection	
Diffractometer	Bruker APEXII CCD
Absorption correction	Multi-scan (<i>SADABS</i> ; Bruker, 2016)
<i>T_{min}</i> , <i>T_{max}</i>	0.677, 0.746
No. of measured, independent and observed [<i>I</i> > 2 σ (<i>I</i>)] reflections	22287, 4253, 2487
<i>R_{int}</i>	0.054
(<i>sin</i> θ / λ) _{max} (Å ⁻¹)	0.649
Refinement	
<i>R</i> [<i>F</i> ² > 2 σ (<i>F</i> ²)], <i>wR</i> (<i>F</i> ²), <i>S</i>	0.060, 0.188, 1.04
No. of reflections	4253
No. of parameters	244
No. of restraints	1
H-atom treatment	H-atom parameters constrained
$\Delta\rho_{max}$, $\Delta\rho_{min}$ (e Å ⁻³)	0.38, -0.25

Computer programs: *APEX3* and *SAINT* (Bruker, 2016), *SHELXT2018/3* (Sheldrick, 2015a), *SHELXL2018/3* (Sheldrick, 2015b), *OLEX2* (Dolomanov *et al.*, 2009), *Mercury* (Macrae *et al.*, 2020), *WinGX* (Farrugia, 2012), *PLATON* (Spek, 2020) and *pubCIF* (Westrip, 2010).

the residue obtained was dissolved in dichloromethane. The organic phase was then dried over Na₂SO₄ and concentrated. The mixture obtained was chromatographed on a silica gel column [eluent: hexane/ethylacetate (2/1)]. The crude product was recrystallized from ethanol as yellow crystals suitable for X-ray analysis (m.p. 493.5 K).

7. Refinement

Crystal data, data collection and structure refinement details are summarized in Table 2. Hydrogen atoms treated as riding: C—H = 0.97 Å and *U*_{iso}(H) = 1.5*U*_{eq}(C) for methyl, C—H = 0.96 Å and *U*_{iso}(H) = 1.2*U*_{eq}(C) for methylene, C—H = 0.93 Å and *U*_{iso}(H) = 1.2*U*_{eq}(C) for aromatic and C—H = 0.98 Å and *U*_{iso}(H) = 1.2*U*_{eq}(C) for methine H atoms.

Funding information

This study was supported by Ondokuz Mayıs University under project No. PYOFEN.1906.19.001.

References

- Abraham, C. J., Paull, D. H., Scerba, M. T., Grebinski, J. W. & Lectka, T. (2006). *J. Am. Chem. Soc.* **128**, 13370–13371.
 Bruker (2016). *APEX3*, *SADABS* and *SAINT*. Bruker AXS Inc., Madison, Wisconsin, USA.
 Burnett, M. N. & Johnson, C. K. (1996). *ORTEP III*. Report ORNL-6895. Oak Ridge National Laboratory, Tennessee, USA.

- Cai, J., Zou, J., Pan, X. & Zhang, W. (2008). *Tetrahedron Lett.* **49**, 7386–7390.
- Dolomanov, O. V., Bourhis, L. J., Gildea, R. J., Howard, J. A. K. & Puschmann, H. (2009). *J. Appl. Cryst.* **42**, 339–341.
- El Janati, A., Elmsellem, H., Kandri Rodi, Y., Ouzidan, Y., Ramdani, M., Mokhtari, M., Abdel-Rahman, I., Cherif Alaoui, I., Ouazzani Chahdi, F. & Kusuma, H. S. (2020). *Int. J. Corros. Scale Inhib.* **9**, 644–660.
- El Janati, A., Kandri Rodi, Y., Jasinski, J. P., Kaur, M., Ouzidan, Y. & Essassi, E. M. (2017). *IUCrData*, **2**, x170901.
- Farrugia, L. J. (2012). *J. Appl. Cryst.* **45**, 849–854.
- Groom, C. R., Bruno, I. J., Lightfoot, M. P. & Ward, S. C. (2016). *Acta Cryst.* **B72**, 171–179.
- Guillon, J., Grellier, P., Labaied, M., Sonnet, P., Léger, J. M., Déprez-Poulain, R., Forfar-Bares, I., Dallemagne, P., Lemaître, N., Péhourcq, F., Rochette, J., Sergheraert, C. & Jarry, C. (2004). *J. Med. Chem.* **47**, 1997–2009.
- Macrae, C. F., Sovago, I., Cottrell, S. J., Galek, P. T. A., McCabe, P., Pidcock, E., Platings, M., Shields, G. P., Stevens, J. S., Towler, M. & Wood, P. A. (2020). *J. Appl. Cryst.* **53**, 226–235.
- Noolvi, M. N., Patel, H. M., Bhardwaj, V. & Chauhan, A. (2011). *Eur. J. Med. Chem.* **46**, 2327–2346.
- Sheldrick, G. M. (2015a). *Acta Cryst.* **A71**, 3–8.
- Sheldrick, G. M. (2015b). *Acta Cryst.* **C71**, 3–8.
- Spek, A. L. (2020). *Acta Cryst.* **E76**, 1–11.
- Turner, M. J., Mckinnon, J. J., Wolff, S. K., Grimwood, D. J., Spackman, P. R., Jayatilaka, D. & Spackman, M. A. (2017). *CrystalExplorer17.5*. The University of Western Australia.
- Westrip, S. P. (2010). *J. Appl. Cryst.* **43**, 920–925.
- Xu, H. & Fan, L. L. (2011). *Eur. J. Med. Chem.* **46**, 1919–1925.
- Yan, L., Liu, F. W., Dai, G. F. & Liu, H. M. (2007). *Bioorg. Med. Chem. Lett.* **17**, 609–612.
- Zouitini, A., Kandri Rodi, Y., Elmselem, H., Ouazzani Chahdi, F., Steli, H., Ad, C., Ouzidan, Y., Essassi, E., Chetouani, A. & Hammouti, B. (2018). *Moroc. J. Chem.* **6**, 391–403.
- Zouitini, A., Kandri Rodi, Y., Ouzidan, Y., Ouazzani Chahdi, F., Mokhtari, M., Abdel-Rahman, I., Essassi, E. M., Aouniti, A., Hammouti, B. & Elmsellem, H. (2019). *Int. J. Corros. Scale Inhib.* **8**, 225–240.

supporting information

Acta Cryst. (2020). E76, 1361-1364 [https://doi.org/10.1107/S2056989020009895]

Synthesis, crystal structures and Hirshfeld surface analysis of 1,4-dibenzyl-6-methyl-1,4-dihydroquinoxaline-2,3-dione

Emine Berrin Cinar, Ayman Zouitini, Youssef Kandri Rodi, Younes Ouzidan, Jérôme Marrot, Damien Prim, Necmi Dege and Eiad Saif

Computing details

Data collection: *APEX3* (Bruker, 2016); cell refinement: *SAINTE* (Bruker, 2016); data reduction: *SAINTE* (Bruker, 2016); program(s) used to solve structure: *SHELXT2018/3* (Sheldrick, 2015a); program(s) used to refine structure: *SHELXL2018/3* (Sheldrick, 2015b); molecular graphics: *OLEX2* (Dolomanov *et al.*, 2009) and *Mercury* (Macrae *et al.*, 2020); software used to prepare material for publication: *WinGX* (Farrugia, 2012), *PLATON* (Spek, 2020), *SHELXL2018* (Sheldrick, 2015b) and *publCIF* (Westrip, 2010).

1,4-Dibenzyl-6-methyl-1,4-dihydroquinoxaline-2,3-dione

Crystal data

$C_{23}H_{20}N_2O_2$

$M_r = 356.41$

Monoclinic, $P2_1/n$

$a = 9.0844$ (12) Å

$b = 18.7227$ (18) Å

$c = 11.2708$ (14) Å

$\beta = 104.848$ (4)°

$V = 1853.0$ (4) Å³

$Z = 4$

$F(000) = 752$

$D_x = 1.278$ Mg m⁻³

Mo $K\alpha$ radiation, $\lambda = 0.71073$ Å

Cell parameters from 4963 reflections

$\theta = 2.6$ – 24.6 °

$\mu = 0.08$ mm⁻¹

$T = 296$ K

Parallelepiped, yellow

$0.30 \times 0.16 \times 0.06$ mm

Data collection

Bruker APEXII CCD
diffractometer

Radiation source: fine-focus sealed tube

φ and ω scans

Absorption correction: multi-scan
(SADABS; Bruker, 2016)

$T_{\min} = 0.677$, $T_{\max} = 0.746$

22287 measured reflections

4253 independent reflections

2487 reflections with $I > 2\sigma(I)$

$R_{\text{int}} = 0.054$

$\theta_{\max} = 27.5$ °, $\theta_{\min} = 2.2$ °

$h = -10 \rightarrow 11$

$k = -17 \rightarrow 24$

$l = -14 \rightarrow 14$

Refinement

Refinement on F^2

Least-squares matrix: full

$R[F^2 > 2\sigma(F^2)] = 0.060$

$wR(F^2) = 0.188$

$S = 1.04$

4253 reflections

244 parameters

1 restraint

Primary atom site location: structure-invariant
direct methods

Secondary atom site location: difference Fourier
map

Hydrogen site location: inferred from
neighbouring sites

H-atom parameters constrained
 $w = 1/[\sigma^2(F_o^2) + (0.0761P)^2 + 0.7497P]$
 where $P = (F_o^2 + 2F_c^2)/3$

$(\Delta/\sigma)_{\max} < 0.001$
 $\Delta\rho_{\max} = 0.38 \text{ e } \text{Å}^{-3}$
 $\Delta\rho_{\min} = -0.24 \text{ e } \text{Å}^{-3}$

Special details

Geometry. All esds (except the esd in the dihedral angle between two l.s. planes) are estimated using the full covariance matrix. The cell esds are taken into account individually in the estimation of esds in distances, angles and torsion angles; correlations between esds in cell parameters are only used when they are defined by crystal symmetry. An approximate (isotropic) treatment of cell esds is used for estimating esds involving l.s. planes.

Fractional atomic coordinates and isotropic or equivalent isotropic displacement parameters (Å^2)

	x	y	z	$U_{\text{iso}}^*/U_{\text{eq}}$
O1	0.6364 (2)	0.24430 (9)	0.60030 (16)	0.0668 (5)
O2	0.6604 (2)	0.34222 (11)	0.77924 (17)	0.0787 (6)
C1	0.3801 (2)	0.42320 (11)	0.5380 (2)	0.0453 (5)
C2	0.2840 (3)	0.48294 (13)	0.5167 (2)	0.0565 (6)
H2	0.290850	0.516663	0.578499	0.068*
C3	0.1779 (3)	0.49239 (14)	0.4035 (3)	0.0606 (7)
C4	0.1685 (3)	0.44202 (16)	0.3149 (3)	0.0665 (7)
H4	0.096780	0.447513	0.240048	0.080*
C5	0.2611 (3)	0.38383 (14)	0.3329 (2)	0.0605 (7)
H5	0.253041	0.350819	0.269920	0.073*
C6	0.3690 (2)	0.37294 (12)	0.4457 (2)	0.0463 (5)
C7	0.0744 (4)	0.55686 (17)	0.3816 (3)	0.0857 (9)
H7A	0.097017	0.586438	0.453541	0.129*
H7B	0.090205	0.583627	0.313222	0.129*
H7C	-0.029766	0.541485	0.364004	0.129*
N1	0.4634 (2)	0.31227 (10)	0.46724 (17)	0.0479 (5)
C8	0.5589 (3)	0.29843 (12)	0.5791 (2)	0.0502 (6)
C9	0.5729 (3)	0.35335 (13)	0.6795 (2)	0.0530 (6)
N2	0.4870 (2)	0.41352 (10)	0.65252 (17)	0.0477 (5)
C10	0.4593 (3)	0.25871 (12)	0.3703 (2)	0.0564 (6)
H10A	0.356426	0.255943	0.318086	0.068*
H10B	0.484757	0.212320	0.408395	0.068*
C11	0.5669 (3)	0.27494 (12)	0.2918 (2)	0.0520 (6)
C12	0.7141 (3)	0.29739 (15)	0.3413 (3)	0.0682 (7)
H12	0.746539	0.306858	0.424992	0.082*
C13	0.8143 (4)	0.30607 (17)	0.2690 (3)	0.0839 (10)
H13	0.913384	0.321355	0.303781	0.101*
C14	0.7672 (5)	0.29203 (17)	0.1452 (4)	0.0907 (11)
H14	0.834725	0.297218	0.096117	0.109*
C15	0.6232 (6)	0.2708 (2)	0.0954 (3)	0.1045 (12)
H15	0.590820	0.262012	0.011500	0.125*
C16	0.5229 (4)	0.26191 (17)	0.1682 (3)	0.0820 (9)
H16	0.423893	0.246823	0.132573	0.098*
C23	0.5078 (3)	0.46790 (13)	0.7488 (2)	0.0561 (6)
H23A	0.502294	0.514721	0.711069	0.067*
H23B	0.608828	0.462678	0.803360	0.067*

C24	0.3920 (3)	0.46424 (11)	0.8239 (2)	0.0486 (5)
C25	0.3412 (3)	0.52590 (13)	0.8661 (2)	0.0641 (7)
H25	0.373901	0.569841	0.844097	0.077*
C26	0.2429 (4)	0.52371 (16)	0.9403 (3)	0.0785 (9)
H26	0.208237	0.565956	0.967137	0.094*
C27	0.1958 (4)	0.45942 (18)	0.9747 (3)	0.0799 (9)
H27	0.129675	0.457886	1.025374	0.096*
C28	0.2455 (4)	0.39791 (16)	0.9349 (3)	0.0777 (8)
H28	0.214200	0.354182	0.959034	0.093*
C29	0.3424 (3)	0.39995 (13)	0.8588 (3)	0.0666 (7)
H29	0.374561	0.357497	0.830698	0.080*

Atomic displacement parameters (Å²)

	U^{11}	U^{22}	U^{33}	U^{12}	U^{13}	U^{23}
O1	0.0702 (12)	0.0659 (11)	0.0686 (12)	0.0218 (9)	0.0256 (9)	0.0050 (8)
O2	0.0710 (13)	0.1036 (15)	0.0554 (11)	0.0349 (11)	0.0050 (10)	−0.0041 (10)
C1	0.0359 (11)	0.0508 (12)	0.0539 (14)	0.0000 (9)	0.0197 (10)	0.0130 (10)
C2	0.0536 (14)	0.0563 (13)	0.0671 (16)	0.0013 (11)	0.0292 (13)	0.0090 (12)
C3	0.0433 (13)	0.0678 (15)	0.0736 (18)	0.0060 (11)	0.0204 (13)	0.0259 (14)
C4	0.0497 (15)	0.089 (2)	0.0604 (16)	0.0034 (14)	0.0131 (12)	0.0162 (15)
C5	0.0476 (14)	0.0820 (17)	0.0528 (15)	−0.0043 (13)	0.0149 (12)	0.0033 (13)
C6	0.0370 (11)	0.0550 (12)	0.0514 (13)	−0.0041 (10)	0.0197 (10)	0.0057 (10)
C7	0.071 (2)	0.090 (2)	0.094 (2)	0.0186 (17)	0.0178 (17)	0.0233 (18)
N1	0.0414 (10)	0.0542 (11)	0.0525 (12)	−0.0031 (8)	0.0200 (9)	0.0006 (9)
C8	0.0458 (13)	0.0563 (13)	0.0540 (14)	0.0056 (11)	0.0231 (11)	0.0057 (11)
C9	0.0449 (13)	0.0656 (15)	0.0518 (14)	0.0104 (11)	0.0184 (12)	0.0029 (11)
N2	0.0442 (10)	0.0510 (10)	0.0519 (11)	0.0002 (8)	0.0194 (9)	−0.0012 (8)
C10	0.0487 (14)	0.0588 (14)	0.0650 (16)	−0.0127 (11)	0.0204 (12)	−0.0112 (12)
C11	0.0514 (14)	0.0517 (12)	0.0570 (14)	0.0012 (11)	0.0213 (11)	−0.0011 (11)
C12	0.0526 (15)	0.0883 (19)	0.0666 (17)	−0.0084 (14)	0.0205 (13)	0.0175 (14)
C13	0.0586 (17)	0.087 (2)	0.117 (3)	0.0116 (15)	0.0420 (18)	0.0379 (19)
C14	0.116 (3)	0.0689 (18)	0.117 (3)	0.0319 (19)	0.084 (3)	0.0182 (18)
C15	0.143 (4)	0.109 (3)	0.082 (2)	−0.003 (3)	0.066 (3)	−0.024 (2)
C16	0.087 (2)	0.094 (2)	0.0682 (19)	−0.0083 (17)	0.0272 (16)	−0.0236 (16)
C23	0.0534 (14)	0.0531 (13)	0.0644 (15)	−0.0076 (11)	0.0198 (12)	−0.0054 (11)
C24	0.0478 (13)	0.0474 (12)	0.0513 (13)	−0.0012 (10)	0.0142 (10)	−0.0025 (10)
C25	0.0786 (19)	0.0498 (13)	0.0684 (17)	0.0069 (12)	0.0272 (15)	−0.0007 (12)
C26	0.099 (2)	0.0731 (18)	0.0750 (19)	0.0230 (17)	0.0426 (17)	−0.0042 (15)
C27	0.082 (2)	0.106 (2)	0.0638 (18)	0.0093 (18)	0.0411 (16)	0.0004 (17)
C28	0.090 (2)	0.0710 (18)	0.085 (2)	−0.0113 (16)	0.0457 (17)	0.0041 (15)
C29	0.0773 (18)	0.0492 (13)	0.0837 (19)	−0.0066 (12)	0.0396 (15)	−0.0059 (13)

Geometric parameters (Å, °)

O1—C8	1.222 (3)	C16—H16	0.9300
O2—C9	1.217 (3)	C15—C14	1.345 (5)
C1—C6	1.388 (3)	C15—H15	0.9300

C1—C2	1.401 (3)	C14—C13	1.376 (5)
C1—N2	1.414 (3)	C14—H14	0.9300
C2—C3	1.400 (4)	C13—C12	1.378 (4)
C2—H2	0.9300	C13—H13	0.9300
C3—C4	1.360 (4)	C12—H12	0.9300
C3—C7	1.511 (4)	C23—C24	1.511 (3)
C4—C5	1.360 (4)	C23—H23A	0.9700
C4—H4	0.9300	C23—H23B	0.9700
C5—C6	1.407 (3)	C24—C25	1.373 (3)
C5—H5	0.9300	C24—C29	1.378 (3)
C6—N1	1.406 (3)	C29—C28	1.378 (4)
N1—C8	1.359 (3)	C29—H29	0.9300
N1—C10	1.476 (3)	C28—C27	1.355 (4)
C8—C9	1.510 (3)	C28—H28	0.9300
C9—N2	1.360 (3)	C27—C26	1.366 (4)
N2—C23	1.464 (3)	C27—H27	0.9300
C10—C11	1.507 (3)	C26—C25	1.371 (4)
C10—H10A	0.9700	C26—H26	0.9300
C10—H10B	0.9700	C25—H25	0.9300
C11—C16	1.370 (4)	C7—H7A	0.9600
C11—C12	1.376 (4)	C7—H7B	0.9600
C16—C15	1.384 (5)	C7—H7C	0.9600
C6—C1—C2	119.4 (2)	C14—C15—C16	120.4 (3)
C6—C1—N2	119.92 (19)	C14—C15—H15	119.8
C2—C1—N2	120.7 (2)	C16—C15—H15	119.8
C3—C2—C1	120.7 (2)	C15—C14—C13	119.7 (3)
C3—C2—H2	119.7	C15—C14—H14	120.1
C1—C2—H2	119.7	C13—C14—H14	120.1
C4—C3—C2	118.7 (2)	C14—C13—C12	119.8 (3)
C4—C3—C7	121.0 (3)	C14—C13—H13	120.1
C2—C3—C7	120.3 (3)	C12—C13—H13	120.1
C5—C4—C3	121.7 (3)	C11—C12—C13	121.1 (3)
C5—C4—H4	119.1	C11—C12—H12	119.4
C3—C4—H4	119.1	C13—C12—H12	119.4
C4—C5—C6	120.8 (3)	N2—C23—C24	114.05 (18)
C4—C5—H5	119.6	N2—C23—H23A	108.7
C6—C5—H5	119.6	C24—C23—H23A	108.7
C1—C6—N1	119.6 (2)	N2—C23—H23B	108.7
C1—C6—C5	118.6 (2)	C24—C23—H23B	108.7
N1—C6—C5	121.7 (2)	H23A—C23—H23B	107.6
C8—N1—C6	122.01 (19)	C25—C24—C29	118.2 (2)
C8—N1—C10	116.47 (19)	C25—C24—C23	120.0 (2)
C6—N1—C10	121.47 (19)	C29—C24—C23	121.7 (2)
O1—C8—N1	122.6 (2)	C28—C29—C24	120.7 (2)
O1—C8—C9	118.9 (2)	C28—C29—H29	119.7
N1—C8—C9	118.5 (2)	C24—C29—H29	119.7
O2—C9—N2	123.4 (2)	C27—C28—C29	120.2 (3)

O2—C9—C8	119.1 (2)	C27—C28—H28	119.9
N2—C9—C8	117.6 (2)	C29—C28—H28	119.9
C9—N2—C1	122.08 (19)	C28—C27—C26	120.0 (3)
C9—N2—C23	116.9 (2)	C28—C27—H27	120.0
C1—N2—C23	121.01 (19)	C26—C27—H27	120.0
N1—C10—C11	113.57 (18)	C27—C26—C25	119.9 (2)
N1—C10—H10A	108.9	C27—C26—H26	120.0
C11—C10—H10A	108.9	C25—C26—H26	120.0
N1—C10—H10B	108.9	C26—C25—C24	121.0 (2)
C11—C10—H10B	108.9	C26—C25—H25	119.5
H10A—C10—H10B	107.7	C24—C25—H25	119.5
C16—C11—C12	117.8 (2)	C3—C7—H7A	109.5
C16—C11—C10	119.8 (2)	C3—C7—H7B	109.5
C12—C11—C10	122.2 (2)	H7A—C7—H7B	109.5
C11—C16—C15	121.2 (3)	C3—C7—H7C	109.5
C11—C16—H16	119.4	H7A—C7—H7C	109.5
C15—C16—H16	119.4	H7B—C7—H7C	109.5
C6—C1—C2—C3	-0.2 (3)	C6—C1—N2—C9	-5.1 (3)
N2—C1—C2—C3	-179.82 (19)	C2—C1—N2—C9	174.47 (19)
C1—C2—C3—C4	0.8 (3)	C6—C1—N2—C23	176.09 (18)
C1—C2—C3—C7	179.8 (2)	C2—C1—N2—C23	-4.3 (3)
C2—C3—C4—C5	-1.3 (4)	C8—N1—C10—C11	-93.4 (2)
C7—C3—C4—C5	179.7 (2)	C6—N1—C10—C11	88.9 (2)
C3—C4—C5—C6	1.2 (4)	N1—C10—C11—C16	-141.3 (2)
C2—C1—C6—N1	-178.95 (18)	N1—C10—C11—C12	44.0 (3)
N2—C1—C6—N1	0.6 (3)	C12—C11—C16—C15	0.2 (4)
C2—C1—C6—C5	0.1 (3)	C10—C11—C16—C15	-174.7 (3)
N2—C1—C6—C5	179.71 (18)	C11—C16—C15—C14	0.5 (5)
C4—C5—C6—C1	-0.6 (3)	C16—C15—C14—C13	-1.0 (5)
C4—C5—C6—N1	178.5 (2)	C15—C14—C13—C12	0.8 (5)
C1—C6—N1—C8	4.6 (3)	C16—C11—C12—C13	-0.4 (4)
C5—C6—N1—C8	-174.4 (2)	C10—C11—C12—C13	174.4 (2)
C1—C6—N1—C10	-177.85 (18)	C14—C13—C12—C11	-0.1 (4)
C5—C6—N1—C10	3.1 (3)	C9—N2—C23—C24	-96.7 (2)
C6—N1—C8—O1	176.7 (2)	C1—N2—C23—C24	82.2 (2)
C10—N1—C8—O1	-1.0 (3)	N2—C23—C24—C25	-144.8 (2)
C6—N1—C8—C9	-5.3 (3)	N2—C23—C24—C29	39.5 (3)
C10—N1—C8—C9	177.02 (19)	C25—C24—C29—C28	-0.6 (4)
O1—C8—C9—O2	-0.4 (3)	C23—C24—C29—C28	175.1 (3)
N1—C8—C9—O2	-178.5 (2)	C24—C29—C28—C27	1.2 (5)
O1—C8—C9—N2	179.0 (2)	C29—C28—C27—C26	-0.6 (5)
N1—C8—C9—N2	0.9 (3)	C28—C27—C26—C25	-0.4 (5)
O2—C9—N2—C1	-176.4 (2)	C27—C26—C25—C24	1.0 (5)
C8—C9—N2—C1	4.2 (3)	C29—C24—C25—C26	-0.4 (4)
O2—C9—N2—C23	2.4 (3)	C23—C24—C25—C26	-176.2 (3)
C8—C9—N2—C23	-176.91 (19)		

Hydrogen-bond geometry (Å, °)

Cg3 is the centroid of the C11–C16 benzene ring.

<i>D</i> —H··· <i>A</i>	<i>D</i> —H	H··· <i>A</i>	<i>D</i> ··· <i>A</i>	<i>D</i> —H··· <i>A</i>
C10—H10 <i>A</i> ···O2 ⁱ	0.97	2.52	3.251 (3)	132
C16—H16···O1 ⁱ	0.93	2.55	3.3984 (4)	152
C25—H25···Cg3 ⁱⁱ	0.93	2.83	3.683 (3)	153

Symmetry codes: (i) $x-1/2, -y+1/2, z-1/2$; (ii) $-x+2, -y, -z$.